

Supporting Information

Microgel enhanced double network hydrogel electrode with high conductivity and stability for intrinsically stretchable and flexible all-gel-state supercapacitor

Yu Zhao[†], Shuo Chen[†], Jian Hu[‡], Jiali Yu[†], Gengchao Feng[§], Bo Yang[†], Cuihua, Li[†], Ning Zhao[#], Caizhen Zhu^{†} and Jian Xu[#]*

[†]College of Chemistry and Environmental Engineering, Shenzhen University, Shenzhen 518060, China

[‡]State Key Lab for Strength and Vibration of Mechanical Structures, Department of Engineering Mechanics, Xi'an Jiaotong University, Xi'an 710049, China

[§]ShenZhen Surg Science Medical Tech. Co., Ltd. Shenzhen 518012, China

[#]Beijing National Laboratory for Molecular Sciences, Institute of Chemistry, Chinese Academy of Sciences, Beijing 100190, PR China

Corresponding Author

* E-mail: czzhu@szu.edu.cn

Experimental Section

Chemicals. Acrylamide (AAM, MACKLIN Industries, Ltd) was recrystallized from chloroform. N, N'-methylenebis(acrylamide) (MBAA, MACKLIN Industries, Ltd) was recrystallized from ethanol. Pyrrole (py, MACKLIN Industries, Ltd) was used after vacuum distillation. Poly (3, 4-ethylenedioxythiophene) polystyrene sulfonate (PEDOT), and potassium peroxydisulfate (KPS) were purchased from MACKLIN Industries, Ltd and used as received.

Fabrication of microgel. The PEDOT was added in a pre-gel solution containing 1 M of AAM monomer, 4 mol % of MBAA as cross-linker, 0.1 mol % KPS as initiator dissolved in deionized water (the molar percentage are respective to the monomer). Then the pre-gel solution was pulled into the cell mold, containing a pair of glasses with silica spacer. The hydrogel was synthesized by thermal polymerization for 12 h, and then it was pulverized by a pulverizer. The pulverized hydrogel was freeze-dried for 24 h to yield the microgel particle powder.

Fabrication of microgel reinforced PEDOT/PAAm single network hydrogel (MR-PEDOT/PAAm SN hydrogel). The dried microgel powder was added in the pre-gel solution containing 1 M of AAM monomer, 0.5 wt% PEDOT, 0.02 mol % of MBAA as cross-linker, 0.1 mol % KPS as initiator dissolved in deionized water (the molar percentage are respective to the monomer). Then the pre-gel solution was pulled into the cell mold containing a pair of glasses with silica spacer. The mix solution was then polymerized under 70 °C for 12 h. The hydrogel was immersed in deionized water for at least 3 days to remove any unreacted reagents.

Fabrication of microgel reinforced double network hydrogel (MR-PEDOT/PAAm DN hydrogel). The MR-PEDOT/PAAm SN hydrogel was immersed in the second network aqueous solution containing 4 M AAM monomer, 0.02 mol % MBAA and 0.1 mol % KPS for one day until equilibrium was reached. After immersion, the second network was polymerized

in the presence of the first network by thermal irradiation at 70 °C for 12 h to obtain MR-PEDOT/PAAm DN hydrogel. After synthesis, the MR-PEDOT/PAAm DN hydrogel was immersed in deionized water for at least 3 days to remove any unreacted reagents.

Fabrication of microgel reinforced PEDOT/PAAm/PPy double network hydrogel (MR-PEDOT/PAAm/PPy DN hydrogel). The MR-PEDOT/PAAm SN hydrogel was immersed in 0.1 M freshly distilled pyrrole and 0.1 M p-toluene sulfonic acid sodium salt solution for 15 min at room temperature under the protection of nitrogen atmosphere, which was prior to commencing the electrodeposition (0.7V vs Ag/AgCl). Then the similar procedure was followed to the fabrication of MR-PEDOT/PAAm DN hydrogel.

Fabrication of stretchable and flexible hydrogel supercapacitor. Polymeric hydrogel electrolyte of PAAm/KCl was polymerized under UV, using AAm as the monomer, MBAA as cross-linker. Two pieces of MR-PEDOT/PAAm DN hydrogel were immersed in 1 M KCl solution. Finally, MR-PEDOT/PAAm DN hydrogel electrodes and PAAm/KCl hydrogel electrolytes were stacked together to form a hydrogel supercapacitor.

Mechanical test. The fracture stress σ_f and the elastic modulus E were determined by the tensile test, which was performed with a commercial test machine. The fully-swollen samples were cut into a dumbbell shape as standardized JIS-K6251-7 size (35 mm long, 2mm wide, gauge length of 12mm and 0.1-0.5 mm thick) with a hydrogel cutting machine. All the samples were stretched at a constant velocity of 100 mm/min. The elastic modulus was determined from the slope of the stress-strain curve within the initial linear region ($0 < \varepsilon < 0.1$, where ε is the strain). The work of extension W_{ext} (MJ/m³) was determined from the area under the stress-strain curve.

Characterization of the electrochemical performance. The hydrogel was cut into pieces (2cm x 2cm, mass loading of active materials is 0.35mg), then a three-electrode electrochemical cell method was used to measure the electrochemical performance with cyclic voltammetry (CV) and galvanostatic charge-discharge (GCD) behavior. The reference electrode was

Ag/AgCl, while the counter electrode was Pt wire. KCl aqueous (1 M) solution was used as the electrolyte for the electrochemical performance test. CV was conducted in a potential range from -0.7 to 0.7 V with a scan rate of 5, 10, 20, 50 and 100 mV s⁻¹, respectively. GCD test was performed at various current densities from 0.5 to 10 A g⁻¹ with the potential window between 0 and 0.6V. Electrochemical impedance spectra (EIS) was measured over the frequency range of 0.01 to 100 kHz.

The specific capacitances C_m are calculated from GCD and CV curves via the following equations

$$C_m = \frac{1}{U_{vm}} \int i(U) dU \quad (1)$$

$$C_m = \frac{It}{Um} \quad (2)$$

Where I is the discharge current during GCD, t is the discharge time during GCD, U is the volume range, m is the mass of electrochemically active materials, v is the scan rate of CV curve and $i(U)$ is the current during CV.

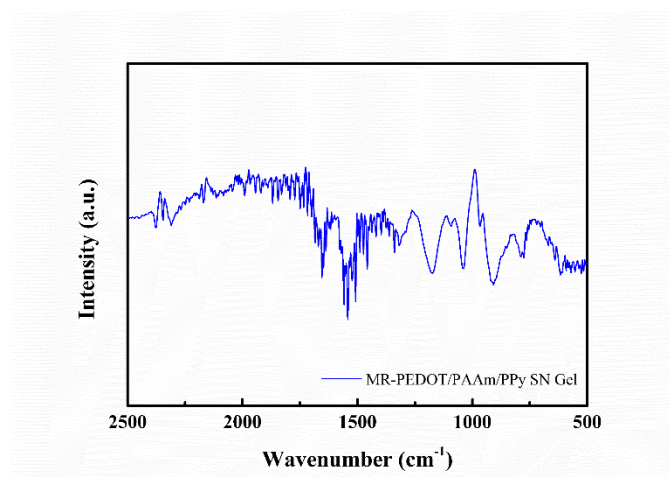


Figure S1. FT-IR spectrum of MR-PEDOT/PAAm/PPy SN gel.

The bands centered at 1560 cm⁻¹, 972 cm⁻¹, 1489 cm⁻¹ and 1458 cm⁻¹ are attributed to the stretching vibration of the C-C double bond, C-C single bond, and C-N bond of PPy, respectively. The band centered at 1039 cm⁻¹ is the stretching vibration of the S=O bond of PEDOT.

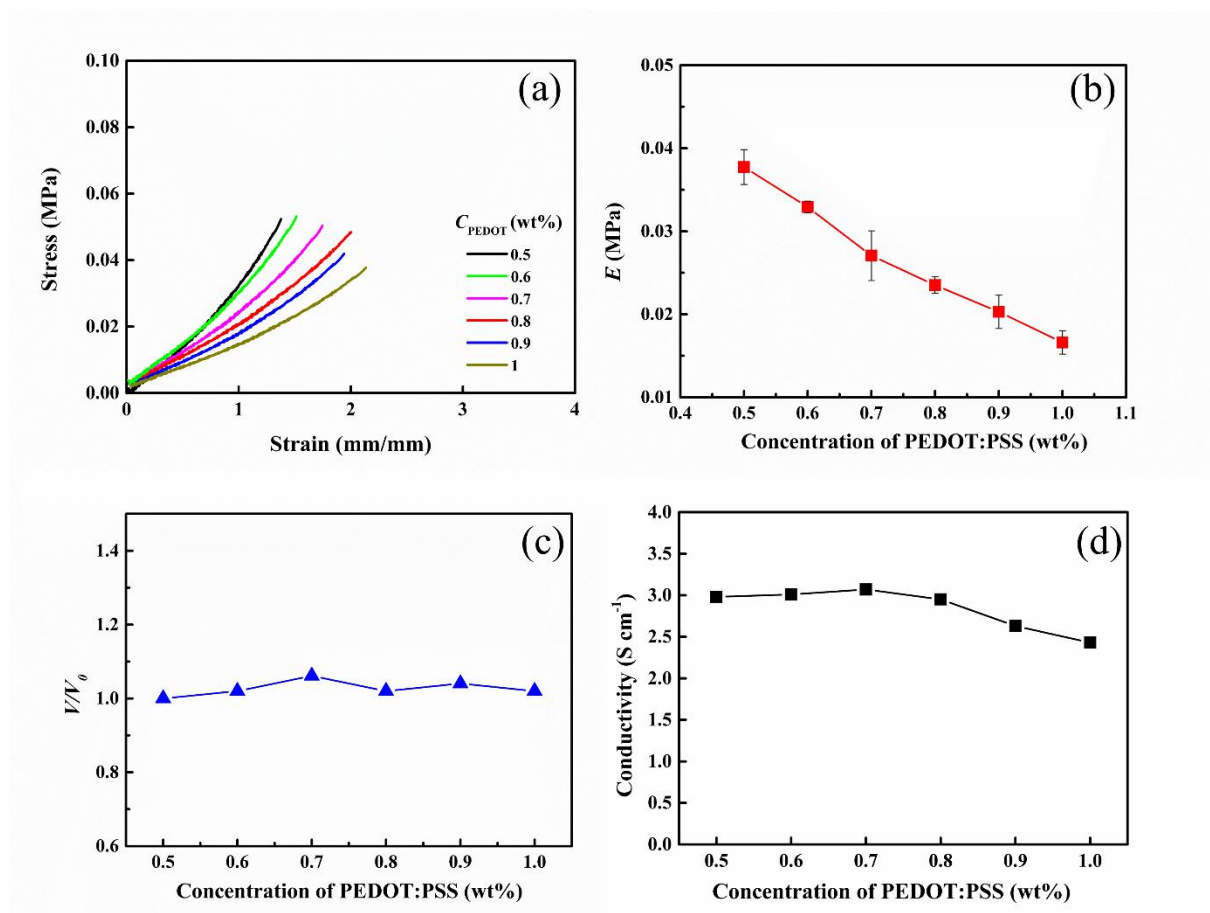


Figure S2. The effect of the PEDOT concentration on the stress-strain curves of MR-PEDOT/PAAm SN hydrogels (a), modulus E (b) and volume change V/V_0 (c), state, conductivity(d), where V_0 is the volume of as-prepared hydrogel and V is the volume of the hydrogel in equilibrium swollen. The hydrogel is synthesized using 1 M PAAm and 0.07 g/mL microgel.

Morphology of hydrogels

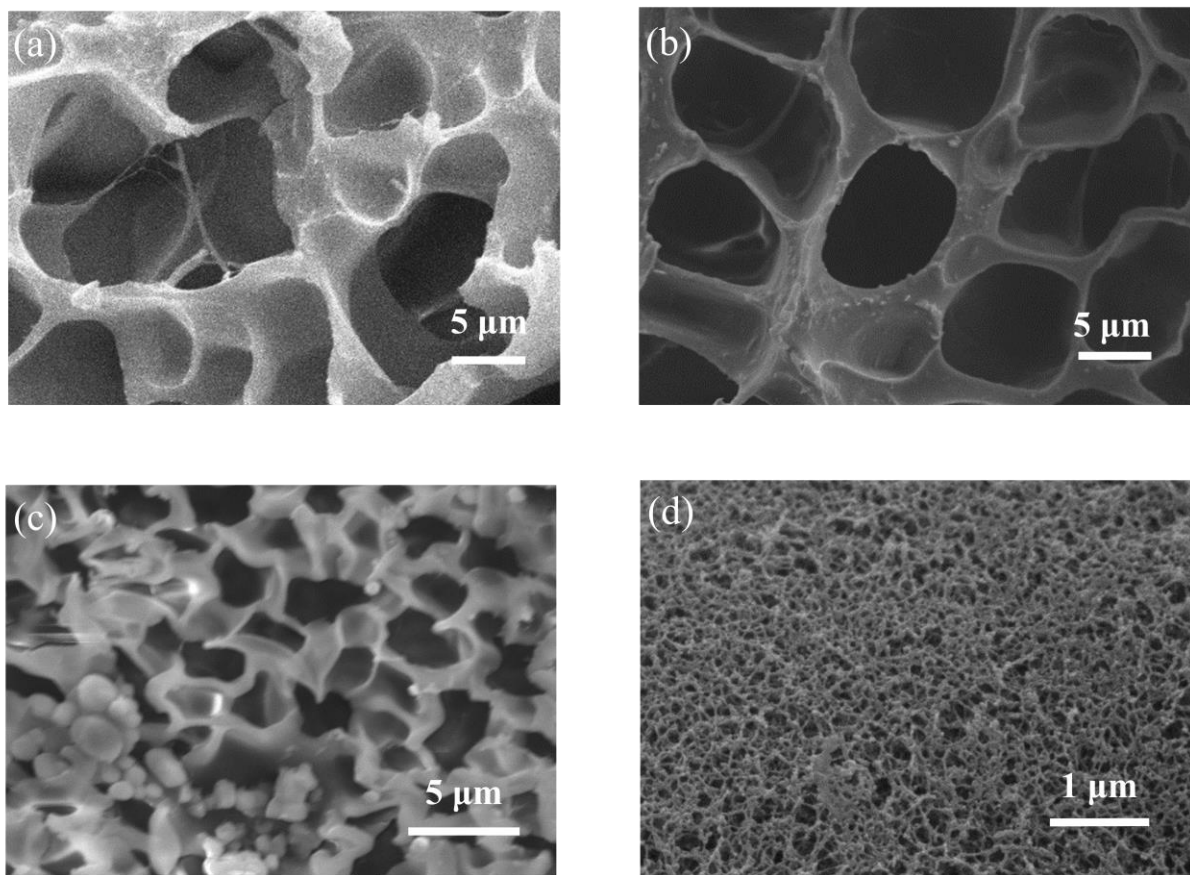


Figure S3. SEM images of PAAm hydrogel (a), PEDOT/PAAm SN hydrogel (b), MR-PEDOT/PAAm SN hydrogel (c) and MR-PEDOT/PAAm/PPy SN hydrogel (d).

The size of network dramatically decreased, while microgel was embedded in the first network, as shown in **Figure S3c**. The results indicated that the loose first network trapped in microgel to form a densely cross-linked network. We found a dense network that fully filled in the previous network after PPy electrodeposition.

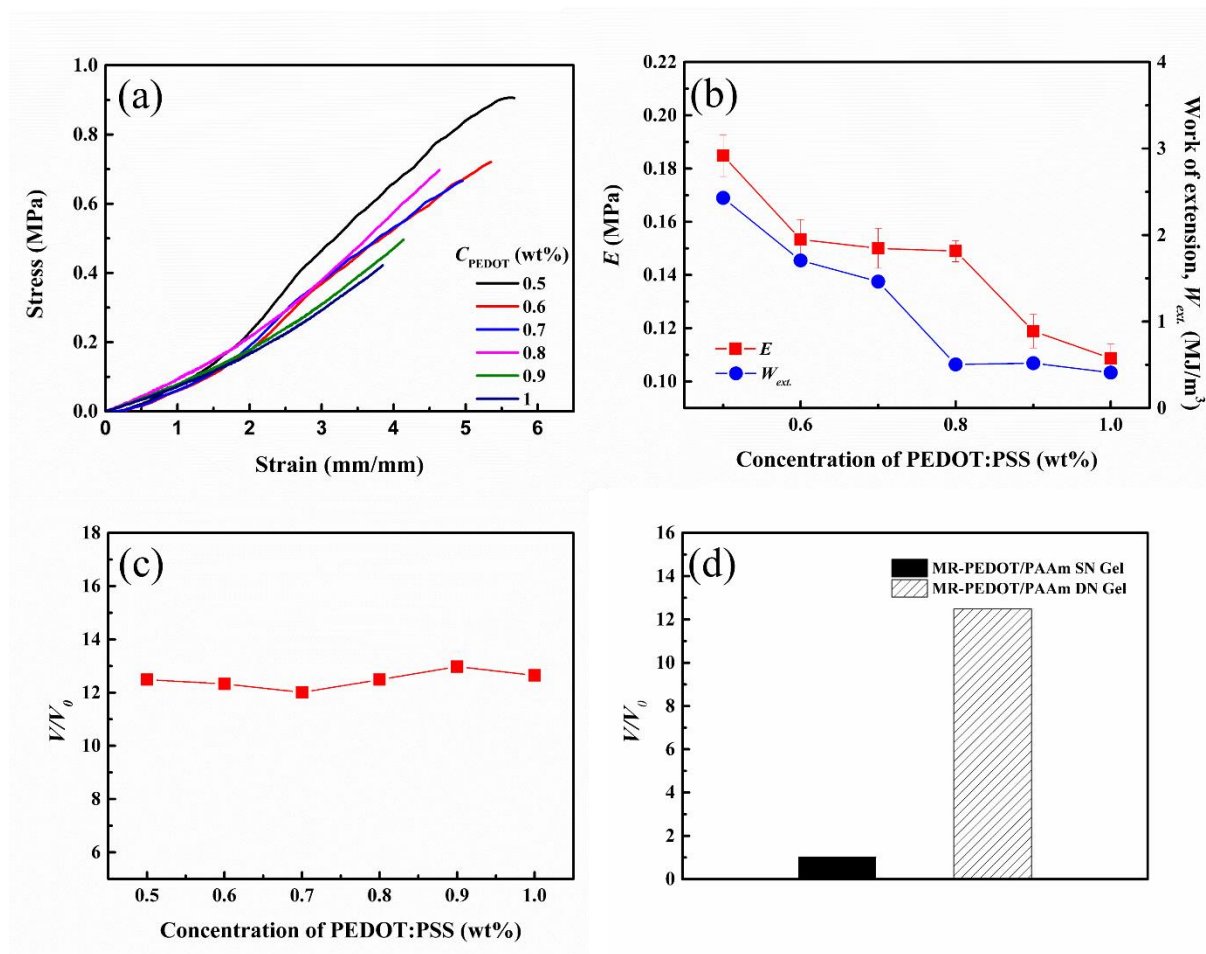


Figure S4. The effect of PEDOT concentration on the tensile stress-strain curves of MR-PEDOT/PAAm DN hydrogels (a), the elastic modulus E and work of extension W_{ext} (b), the volume swelling ratio V/V_0 , where V_0 is the volume of as-prepared single network hydrogel and V is the volume of DN hydrogel in equilibrium swollen state (c). The comparison of V/V_0 of volume swelling ratio MR-PEDOT/PAAm DN hydrogel with MR-PEDOT/PAAm SN hydrogel (d). The first hydrogel network synthesized at 1M PAAm and 0.07 g/ml microgel, and the second AAm monomer concentration is 4 M.

Figure S4a shows the effect of PEDOT on the tensile stress-strain curves of MR-PAAm DN hydrogels with various PEDOT concentrations. The high PEDOT concentration led the low fracture stress and fracture strain. Attributed to the few of the second PAAm polymer interpenetrated microgel, which cannot sustain the large deformation to dissipated energy. Meanwhile, the modulus decreased with the increasing of PEDOT concentration, which was decided by the structure of the first hydrogel network.

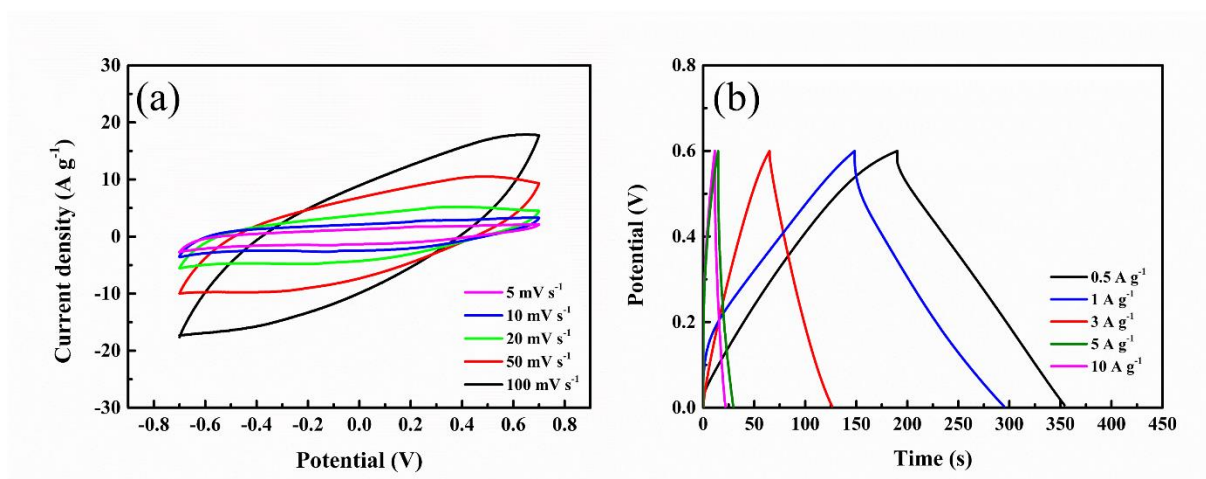


Figure S5. (a) CV curves for MR-PEDOT/PAAm SN hydrogel at scan rates of 5, 10, 20, 50 and 100 mV s⁻¹. (b) GCD curves for MR-PEDOT/PAAm SN hydrogel at different current densities.

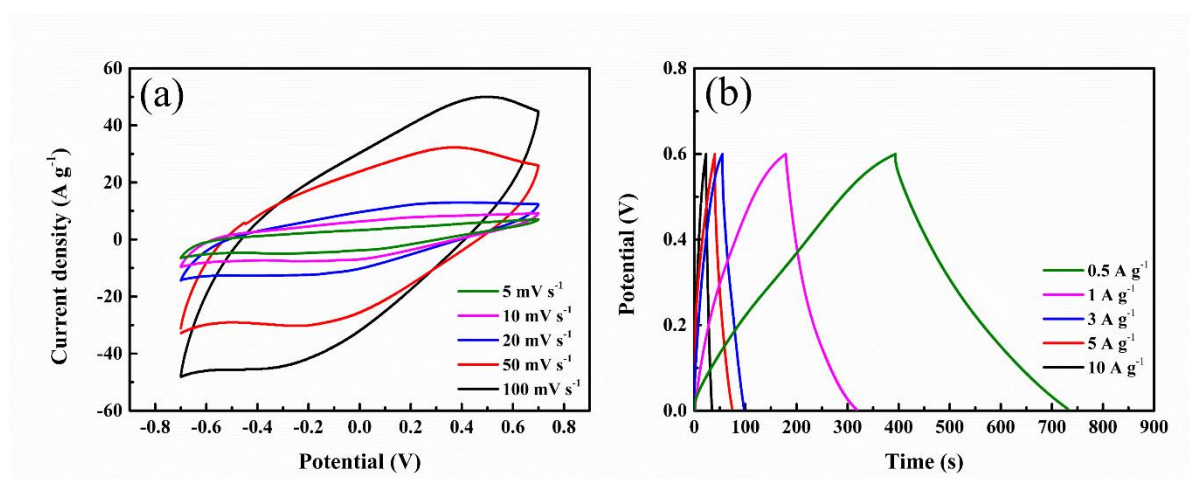


Figure S6. (a) CV curves for MR-PEDOT/PAAm/PPy SN hydrogel at scan rates of 5, 10, 20, 50 and 100 mV s⁻¹. (b) GCD curves for MR-PEDOT/PAAm/PPy SN hydrogel at different current densities.

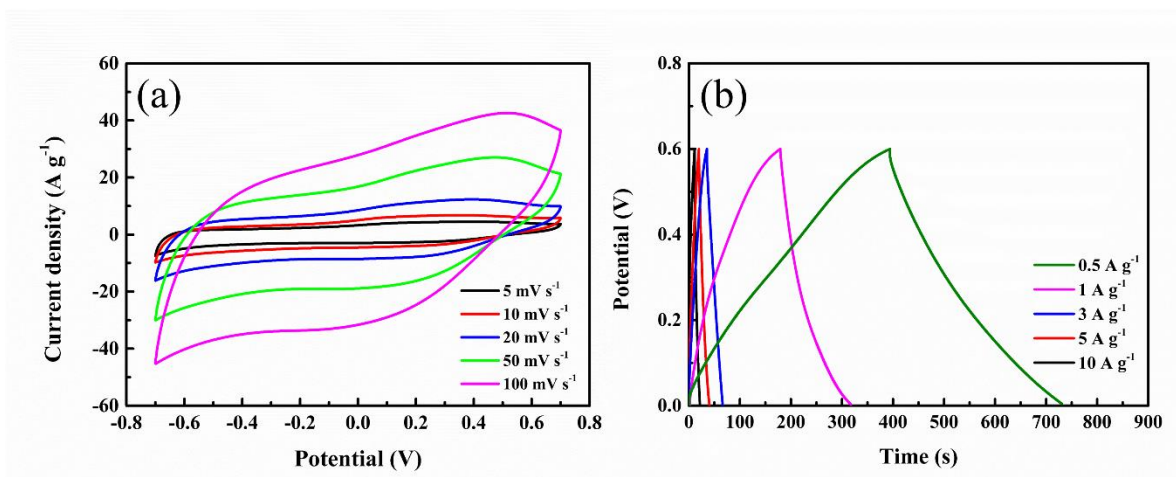


Figure S7. (a) CV curves for MR-PEDOT/PAAm/PPy DN hydrogel at scan rates of 5, 10, 20, 50 and 100 mV s^{-1} . (b) GCD curves for MR-PEDOT/PAAm/PPy DN hydrogel at different current densities.

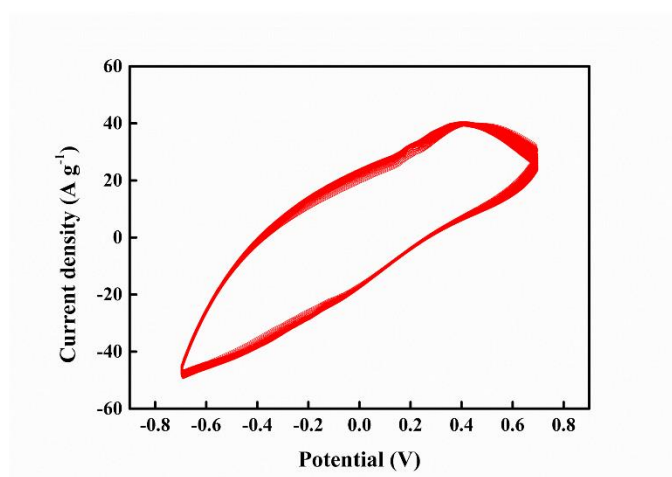


Figure S8. The stability of MR-PEDOT/PAAm/PPy DN hydrogel as an electrode. Cycle performance at a scan rate of 100 mV s^{-1} for 1000 cycles.

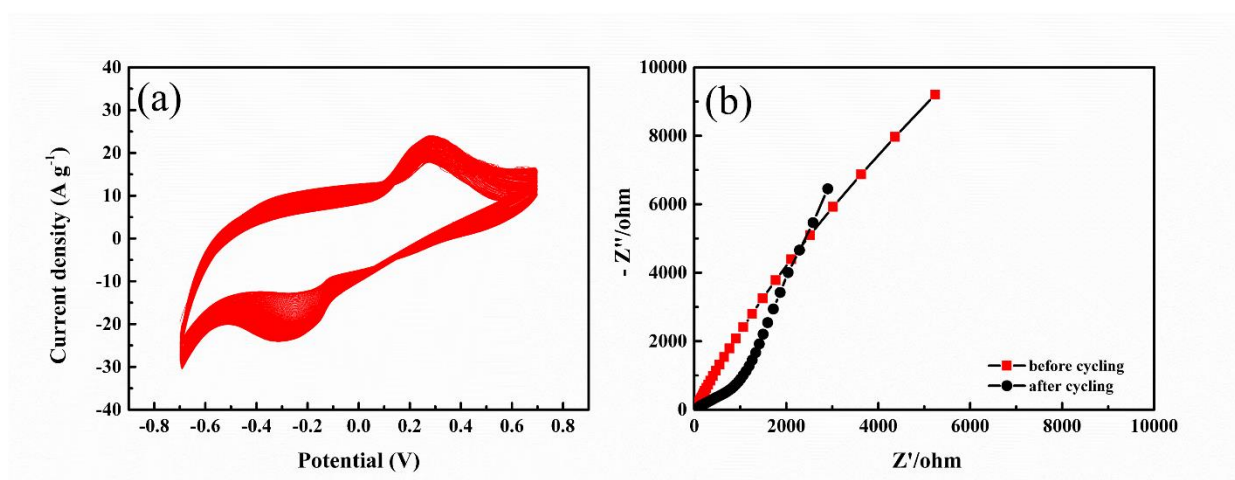


Figure S9. The stability of PEDOT/PAAm/PPy DN gel as an electrode. (a) Cycle performance at a scan rate of 100 mV s^{-1} for 1000 cycles. (b) EIS curves for the electrode before and after cycling.

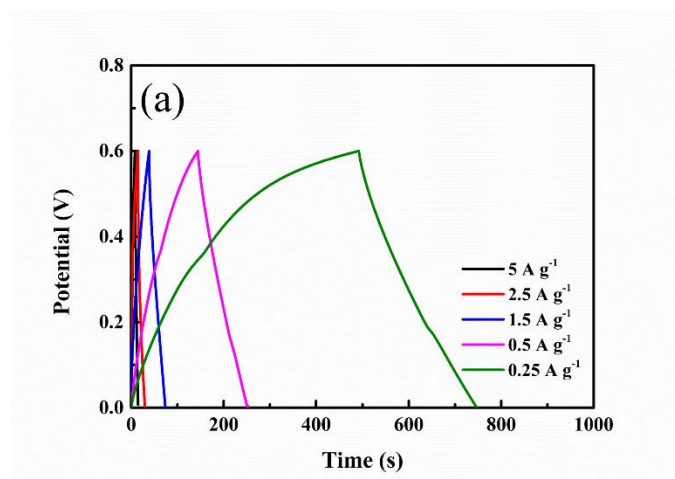


Figure S10. GCD curves for a textile gel supercapacitor at different current densities.

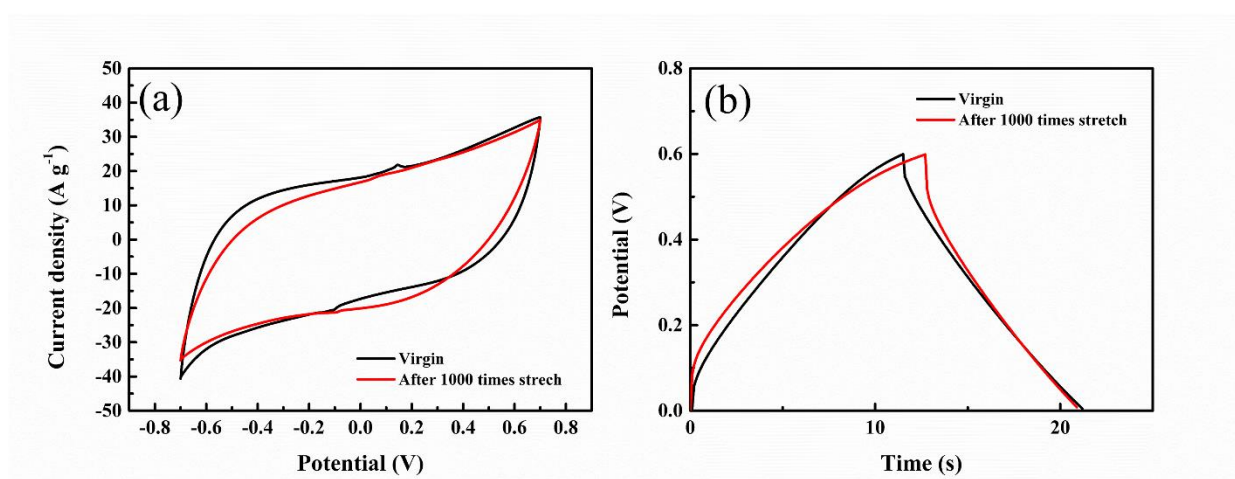


Figure S11. (a) CV curves for a textile gel supercapacitor at a scan rate of 100 mV s^{-1} . (b) GCD curves for a textile gel supercapacitor at a current density of 5 A g^{-1} . The measurements were performed under 1000 times stretch at 100% strain.

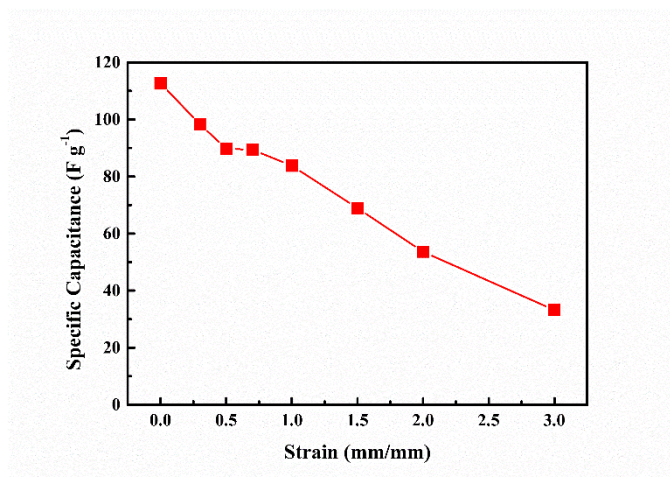


Figure S12. The specific capacitance for a textile gel supercapacitor under various stretch strain calculated from the GCD curves at a current density of 0.5 A g^{-1} .